General parametric analysis of the linear two-stream instability

V. Lapuerta and E. Ahedo
E.T.S.I. Aeronáuticos, Universidad Politécnica de Madrid, 28040 Madrid, Spain

(Received 16 November 2001; accepted 15 January 2002)

A complete and systematic picture of the different forms of the linear two-stream instability is presented. It is based in an asymptotic study of the general solution of the dispersion relation, in terms of the three dimensionless parameters characterizing the steady state of a two-species plasma. In a zero temperature-ratio limit, the parametric regions of dominance of different acoustic, Langmuir, and reactive types of the instability are determined, and analytical expressions of the maximum growth rate for all types are derived. The continuous transition between different types and the main topological changes of the unstable branch, as the parametric space is covered, are discussed. For the small temperature-ratio case, new analytical expressions for the instability threshold are derived. © *2002 American Institute of Physics.* [DOI: 10.1063/1.1464893]

I. INTRODUCTION

Some forms of the two-stream instability for ion–electron $(i-e)$ and electron–electron $(e-e)$ plasmas have been very well known for a long time. These are the ion-acoustic instability[1,2] (for low drift velocities) and the Buneman or reactive instability[3] (for high drift velocities) in an $i-e$ plasma, and the cold-beam (or reactive) and gentle-bump instabilities for an $e-e$ plasma.[2,4] Less common and less known forms of the two-stream instability are the ion-plasma and hot ion-kinetic instabilities for an $i-e$ plasma,[5] and the $e-e$ acoustic instability, originally studied by Gary.[6]

In addition, the knowledge on both the parametric regions of dominance of the different instability types, and the topological changes (of the wave-number-frequency curves) at the transitions between them is incomplete too. On the one side, the evolution from the gentle-bump to the weak-beam $e-e$ instability was studied in detail by O'Neil and Malmberg[7] and Cairns.[8] The evolution from the ion-acoustic to the Buneman instability was studied numerically by Stringer[9] and analytically by us in a recent paper,[10] where we discussed the change from a resistive character associated to the Landau resonance to a reactive character, as the drift velocity increases. On the other side, the parametric domain and properties of the $e-e$ acoustic instability have been investigated numerically mainly, and its dominant character is unclear. In spite of its name, Gary[6] found that the $e-e$ acoustic instability presents a Langmuir character for a certain range of the species density ratio, and Mace and Hellberg[11] found branch mixing between Langmuir and acoustic modes within that instability domain. Finally, the relation between the $e-e$ acoustic and gentle-bump instabilities is poorly understood.

Another issue of great interest is the conditions on the plasma parameters defining the instability threshold. There are numerical computations of the drift velocity at the instability threshold for the $i-e$ instability,[12–14] and for the $e-e$ acoustic and the gentle-bump instabilities.[6,15] Limited analytical expressions of the instability threshold are available for the ion-acoustic instability[1,5] and for the ion-plasma instability.[5,14]

This paper attempts to provide a complete and systematic picture of the different types and characteristics of the two-stream instability. A generic two-species, collisionless, unmagnetized, and homogeneous plasma is considered. That picture will be obtained from an asymptotic analysis of the linear dispersion relation in terms of the three dimensionless parameters characterizing the steady state of the plasma. The analysis determines (i) the parametric regions of dominance of the different stability types, (ii) the evolution in character from one type to another, (iii) analytical expressions for the maximum growth rate and associated wave number, and (iv) analytical expressions for the instability threshold.

The layout of the paper is as follows: In Sec. II we present a complete description of the different instability types from the study of the zero Debye-length-ratio case. In Sec. III we derive analytical expressions of the instability threshold for the three different cases that can arise. Conclusions are presented in Sec. IV.

II. GENERAL DERIVATION OF THE INSTABILITY TYPES

The general form of the plasma dispersion relation in a collisionless plasma, for eigenmodes involving only perturbations of two-species (a and b), drifting with a relative velocity $\mathbf{V}_d$, can be expressed as

$$1+\sum_{\alpha=a,b}\frac{R(z_\alpha)}{k^2\lambda_{D\alpha}^2}\equiv 1+\sum_{\alpha=a,b}\frac{\omega_{p\alpha}^2}{k^2\gamma(z_\alpha)c_\alpha^2-\omega^2}=0. \tag{1}$$

Here,

$$z_a=\frac{\omega-kV_d}{kc_a},\quad z_b=\frac{\omega}{kc_b},$$
$$c_\alpha=\sqrt{\frac{T_\alpha}{m_\alpha}},\quad V_d=\frac{\mathbf{V}_d\cdot\mathbf{k}}{k}, \tag{2}$$

and $R(z)$ and $\gamma(z)=z^2+R^{-1}(z)$ are plasma response functions summarized in the Appendix; the rest of the symbols are conventional.

The steady state of the two-species plasma is characterized by three dimensionless parameters,

$$v_d=\frac{V_d}{c_a},\quad \Omega=\frac{\omega_{pb}}{\omega_{pa}}\equiv\left(\frac{n_b m_a}{n_a m_b}\right)^{1/2},$$
$$\Lambda=\frac{\lambda_{Db}}{\lambda_{Da}}\equiv\left(\frac{n_a T_b}{n_b T_a}\right)^{1/2}\equiv\frac{1}{\Omega}\frac{c_b}{c_a}. \tag{3}$$

We will look for the solutions

$$\omega_{re}+\mathrm{i}\omega_{im}=\omega(k;v_d,\Omega,\Lambda)$$

of Eq. (1), for k real and positive. The eigenmodes of Eq. (1) are grouped in two pairs of branches, which, depending on their (ω_{re},k) characteristics, and except in regions of branch mixing, can be classified into Langmuir and acoustic branches.

The unstable eigenmodes will correspond to $\omega_{im}>0$. For each (Ω,Λ) we will find that there is a minimum drift velocity $v_d=v_{dt}(\Omega,\Lambda)$ for the existence of unstable modes. For each (v_d,Ω,Λ), with $v_d>v_{dt}$, the characteristics of the most unstable mode will be designated with an asterisk as superscript; in particular, the maximum growth-rate will be $\omega_{im}^*(v_d,\Omega,\Lambda)$. By exploiting the different symmetries of Eq. (1), the discussion of its general solution can be reduced, without loss of generality, to the parametric interval

$$0<v_d,\quad 0<\Omega,\quad 0\leqslant\Lambda\leqslant 1.$$

The central point of our analysis is that a complete and clear view of the different stability types of Eq. (1) is obtained from the study of the asymptotic limit $\Lambda\to 0$. Equation (1) can be expressed as

$$\frac{\omega^2}{\omega_{pb}^2}=k^2\lambda_{Da}^2\left(\frac{1}{k^2\lambda_{Da}^2+R(z_a)}+\gamma(z_b)\Lambda^2\right), \tag{4}$$

and, for $\Lambda\to 0$, the last term is negligible and the dispersion relation becomes

$$\frac{\omega^2}{\omega_{pb}^2}=\frac{k^2\lambda_{Da}^2}{k^2\lambda_{Da}^2+R(z_a)}, \tag{5}$$

which depends on v_d and Ω through

$$z_a=\frac{\omega/\omega_{pb}}{k\lambda_{Da}}\Omega-v_d, \tag{6}$$

exclusively.

Equation (5) yields unstable solutions for any $|v_d|\neq 0$, that is

$$v_{dt}(\Omega,\Lambda=0)=0.$$

We demonstrate next that the dominant instability mode of Eq. (5) takes different asymptotic forms in the parametric plane (v_d,Ω). Their approximate regions of dominance are sketched in Fig. 1. To justify these domains, we look for the characteristics of the most unstable mode, investigating successively the cases: (i) $k^*\lambda_{Da}\gg 1$, (ii) $|z_a^*|\ll 1$, (iii) $z_a^*\simeq -v_d$, and (iv) $|z_a^*|\gg 1$.

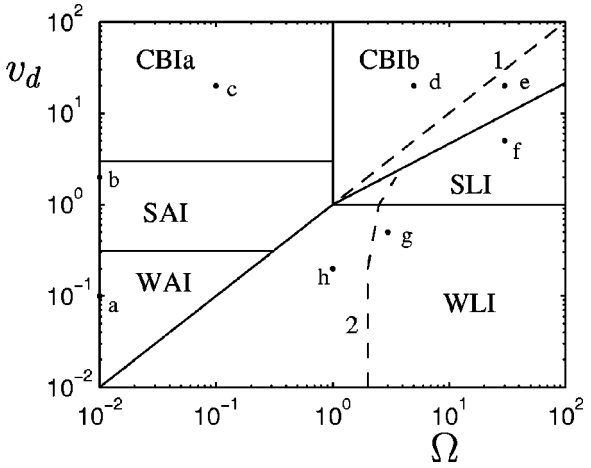

FIG. 1. Approximate domains of dominance of the different types of the two-stream instability for $\Lambda=0$. Dashed line 1 corresponds to the change of character of modes with $k\lambda_{Da}=0$. Dashed line 2 (which coincides with the CBI/SLI transition for $\Omega\gg 1$) locates the branch mixing between acoustic and Langmuir modes. Points a–h refer to plots in Fig. 2.

Modes with $k\lambda_{Da}\gg 1$ in Eq. (5) follow

$$\frac{\omega^2}{\omega_{pb}^2}\simeq 1-\frac{R(z_a)}{k^2\lambda_{Da}^2},$$

which correspond to two Langmuir waves (on a frame tied to species b) with $\omega_{re}\simeq\pm\omega_{pb}$. For $v_d>0$, the branch with ω_{re} positive satisfies

$$\frac{\omega_{im}}{\omega_{pb}}\simeq-\sqrt{\frac{\pi}{8}}z_a\frac{(v_d+z_a)^2}{\Omega^2}\exp\left(-\frac{z_a^2}{2}\right),$$
$$k\lambda_{Da}\simeq\frac{\Omega}{v_d+z_a}, \tag{7}$$

and is unstable for $z_a<0$ (i.e., $k\lambda_{Da}>\Omega/v_d$). Keeping $\Omega/v_d\gg 1$, simple expressions for the maximum growth rate exist for large and small drift velocities. For $1\ll v_d$, we find $z_a^*\simeq -1$, leading to

$$\frac{\omega_{im}^*}{\omega_{pb}}\simeq\sqrt{\frac{\pi}{8\mathrm{e}}}\frac{v_d^2}{\Omega^2},\quad k^*\lambda_{Da}\simeq\frac{\Omega}{v_d}, \tag{8}$$

which we call the strong Langmuir instability (SLI), and corresponds to the gentle-bump instability for $e-e$ plasmas,[2,4] and to the hot-ion kinetic instability for $i-e$ plasmas.[5] Then, for $v_d\ll 1$, we find $z_a^*\simeq -v_d/3$, leading to

$$\frac{\omega_{im}^*}{\omega_{pb}}\simeq\frac{\sqrt{2\pi}}{27}\frac{v_d^3}{\Omega^2},\quad k^*\lambda_{Da}\simeq\frac{3\Omega}{2v_d}, \tag{9}$$

which we call the weak Langmuir instability (WLI), and corresponds to the ion-plasma instability for $i-e$ plasmas,[5] and to part of the $e-e$ acoustic instability of Gary.[6]

The WLI presents $|z_a^*|\ll 1$. We look next for modes with $|z_a|\ll 1$ in Eq. (5). These satisfy

$$\frac{\omega^2}{\omega_{pb}^2}=\frac{k^2\lambda_{Da}^2}{k^2\lambda_{Da}^2+1}\left(1-\frac{\mathrm{i}R_2(z_a)}{1+k^2\lambda_{Da}^2}\right). \tag{10}$$

For $k\lambda_{Da}\ll 1$, these modes constitute two acoustic branches with phase velocities $\omega_{re}/k\simeq\pm\lambda_{Da}\omega_{pb}=\pm c_a/\Omega$. For $v_d>0$ the branch with ω_{re} positive has

$$\frac{\omega_{im}}{\omega_{pb}}\simeq -z_a\sqrt{\frac{\pi}{8}}\frac{k\lambda_{Da}}{(1+k^2\lambda_{Da}^2)^{3/2}},$$
$$z_a\simeq\frac{\Omega}{\sqrt{1+k^2\lambda_{Da}^2}}-v_d, \tag{11}$$

and modes with $z_a<0$ are unstable. Simple expressions for the maximum growth rate are easily found for small and large values of v_d/Ω. For $v_d\ll\Omega$, Eq. (11) yields again Eq. (9) for the WLI. For $\Omega\ll v_d$, we find

$$\frac{\omega_{im}^*}{\omega_{pb}}\simeq\sqrt{\frac{\pi}{54}}v_d,\quad k^*\lambda_{Da}\simeq\frac{1}{\sqrt{2}},\quad z_a^*\simeq -v_d, \tag{12}$$

which we call the weak acoustic instability (WAI), and corresponds to the ion-acoustic instability in $i-e$ plasmas,[2] and to another part of the $e-e$ acoustic instability.[6]

In order to have $|z_a^*|\ll 1$, expressions for the WAI are restricted to $v_d\ll 1$. We next consider eigenmodes of Eq. (5) with $z_a\simeq -v_d$. These modes are quasisteady (as seen in the b-frame) for species a and follow

$$\frac{\omega}{\omega_{pb}}=\pm\frac{k\lambda_{Da}}{\sqrt{k^2\lambda_{Da}^2+R_1(-v_d)+iR_2(-v_d)}}. \tag{13}$$

For $k\lambda_{Da}\ll 1$ and $|v_d|$ not large they can still be considered acoustic branches. For $v_d>0$, the branch with ω_{re} positive is unstable for any k. Of course, the simple expressions of the WAI, Eq. (12), are recovered for $v_d\ll 1$. For $v_d=O(1)$, there are no analytical expressions for ω_{im}^* and $k^*\lambda_{Da}$, but both are of order unity, and we can talk of a strong acoustic instability (SAI). This was discussed by us for an $i-e$ plasma in Ref. 10. For $R_1(v_d)>0$, which corresponds to $v_d<1.31$ (see the Appendix), the SAI is purely resistive, due entirely to the Landau resonance. For $v_d>1.31$, both R_1 and R_2 contribute to the most unstable mode. For $v_d>3$, roughly, $|R_2(v_d)|$ becomes negligible and the quasisteady approximation of Eq. (13) fails because it overestimates ω_{im}^*. Small temporal effects on species a must be taken into account to reproduce correctly the most unstable mode.[10]

For $v_d\gtrsim 3$, we look for modes with $|z_a|\gg 1$. Using the large-argument expansion of $R(z)$ (see the Appendix), Eq. (5) becomes

$$\frac{\omega_{pb}^2}{\omega^2}+\frac{\omega_{pa}^2}{(\omega-kV_d)^2}=1, \tag{14}$$

which corresponds to the reactive or cold-beam instability[4] (CBI) for an $e-e$ plasma, also named Buneman instability[3] for an $i-e$ plasma. The characteristics of the most unstable mode depend on the value of Ω. For $v_d>0$ the most unstable mode satisfies

$$\frac{\omega_{re}^*}{\omega_{pb}}\simeq\frac{1}{2^{4/3}}\frac{1}{\Omega^{1/3}},\quad \frac{\omega_{im}^*}{\omega_{pb}}\simeq\frac{3^{1/2}}{2^{4/3}}\frac{1}{\Omega^{1/3}},$$
$$k^*\lambda_{Da}\simeq\frac{1}{v_d},\quad z_a^*\simeq -v_d, \tag{15}$$

if $\Omega\ll 1$ (type CBIa in Fig. 1),

$$\frac{\omega_{re}^*}{\omega_{pb}}\simeq\frac{\sqrt{3}}{2},\quad \frac{\omega_{im}^*}{\omega_{pb}}\simeq\frac{1}{2},\quad k^*\lambda_{Da}\simeq\frac{\sqrt{3}}{v_d},$$

if $\Omega=1$, and

$$\frac{\omega_{re}^*}{\omega_{pb}}\simeq 1-\frac{1}{2^{4/3}}\frac{1}{\Omega^{2/3}},\quad \frac{\omega_{im}^*}{\omega_{pb}}\simeq\frac{3^{1/2}}{2^{4/3}}\frac{1}{\Omega^{2/3}},$$
$$k^*\lambda_{Da}\simeq\frac{\Omega}{v_d},\quad |z_a^*|\simeq O\left(\frac{v_d}{\Omega^{2/3}}\right), \tag{16}$$

if $\Omega\gg 1$ (type CBIb in Fig. 1). The symmetry between species a and b in Eq. (14) means that modes corresponding to (v_d,Ω) and (v_d,Ω^{-1}) are identical, if one exchanges adequately the role of each species and the spatial reference frame; the differences in expressions (15) and (16) come from using the same nondimensionalization in both cases.

Expression (16) for the CBIb is valid when $\Omega\ll v_d^{3/2}$ (i.e., $|z_a^*|\gg 1$). Parameter $k^*\lambda_{Da}$ grows with Ω, and one has $k^*\lambda_{Da}\gg 1$ at $\Omega\sim v_d^{3/2}$, already in the domain of the SLI, Eq. (8). The transition between the CBIb and the SLI, studied by O'Neil and Malmberg[7] and Cairns,[8] must take place somewhere in the region $v_d<\Omega<v_d^{3/2}$, with $v_d\gg 1$, where both expressions (8) and (16) seem to be valid. The analysis of the dispersion relation

$$\frac{\omega_{pb}^2}{\omega^2}+\frac{\omega_{pa}^2}{(\omega-kv_d)^2}=1+i\frac{R_2(z_a)}{k^2\lambda_{Da}^2}, \tag{17}$$

appropriate to that transition region, shows that the CBI dominates over the SLI whenever $\Omega\ll O(v_d^{3/2})$; the same result is obtained by just equating Eqs. (8) and (16) for ω_{im}^*.

This completes the asymptotic investigation of the two-stream instability in the parametric plane (Ω,v_d) for $\Lambda\to 0$. The regions of dominance of Langmuir [Eq. (7)], acoustic [Eq. (13)], and reactive [Eq. (14)] unstable modes have been identified, and each one presents different asymptotic subtypes. Table I summarizes them; notice that the last row of the table connects with the first row.

Figures 2(a)–2(h) show the topological evolution of $\omega(k)$ for the unstable branch as the parametric plane (Ω,v_d) in Fig. 1 is covered clockwise. The following features are worth noting:

(1) For $k\lambda_{Da}\to 0$ the two Langmuir branches satisfy

$$\omega/\omega_{pb}=\pm\sqrt{1+\Omega^{-2}},$$

and the acoustic branches follow

$$\omega/\omega_{pb}=a_0k\lambda_{Da},$$

where the complex constant a_0 is the solution of

$$a_0^2R(\Omega a_0-v_d)=1,$$

TABLE I. Characteristics of the different types of the two-stream instability for $\Lambda \ll 1$.

Type	Domain	v_{dt}	z_a^*	$k^*\lambda_{Da}^*$	$\omega_{im}^*/\omega_{pb}$
SLI	$1 \ll v_d \ll \Omega^{2/3}$	$\Omega\Lambda\sqrt{-4\ln\Lambda}$	-1	$\frac{\Omega}{v_d}$	$\sqrt{\frac{\pi}{8e}}\frac{v_d^2}{\Omega^2}$
WLI	$v_d \ll 1, v_d \ll \Omega$	$\Omega\Lambda\sqrt{-2\ln(\Lambda^3\Omega)}$	$\ll 1$	$\frac{3\Omega}{2v_d}$	$\frac{\sqrt{2\pi}}{27}\frac{v_d^3}{\Omega^2}$
WAI	$\Omega \ll v_d \ll 1$	$\frac{1}{\Lambda^3}\exp\left(-\frac{1}{2\Lambda^2}\right)$	$\ll 1$	$\frac{1}{\sqrt{2}}$	$\sqrt{\frac{\pi}{54}}v_d$
SAI	$\Omega \ll 1, v_d = O(1)$		$-v_d$	$O(1)$	$O(1)$
CBIa	$\Omega \ll 1, 1 \ll v_d$		$\gg 1$	$\frac{1}{v_d}$	$\frac{\sqrt{3}}{2^{4/3}}\frac{1}{\Omega^{1/3}}$
CBIb	$1 \ll \Omega^{2/3} \ll v_d$		$\gg 1$	$\frac{\Omega}{v_d}$	$\frac{\sqrt{3}}{2^{4/3}}\frac{1}{\Omega^{2/3}}$

with $R(z)$ the plasma dispersion function. One acoustic branch is shown in Figs. 2(a)–2(h), whereas one Langmuir branch is depicted in Figs. 2(d)–2(h) only [for the cases of Figs. 2(a)–2(c), the Langmuir branch departs from $\omega/\omega_{pb} \simeq \Omega^{-1}$].

(2) The acoustic mode is unstable at $k=0$ only for $v_d > \Omega$ [Figs. 2(a)–2(d)]. For $\Omega > v_d$ [Figs. 2(e)–2(h)], modes in the (approximate) range

$$k\lambda_{Da} < (\Omega^2/v_d^2 - 1)^{1/2} \tag{18}$$

are stable. This last result was derived by Jackson[1] for $\Omega \ll 1$, but it is valid for any Ω, as can be justified from Eq. (22) in the next section.

(3) A topological change occurs at the transition from a resistive to a reactive instability [between Figs. 2(b) and 2(c)].[10] The strong coupling between the acoustic and Langmuir branches bounds the unstable modes, instead of the vanishing Landau resonance, and makes modes with

$$k\lambda_{D_a} > v_d^{-1}(1+\Omega^{2/3})^{3/2}$$

stable in Figs. 2(c)–2(e).

(4) There is branch mixing at the transition from the CBI to the SLI [between Figs. 2(e) and 2(f)], at a wave number close to the most unstable mode ($k \simeq k^*$), which was studied extensively by O'Neil and Malmberg,[7] and by Cairns.[8]

(5) There is a second branch mixing, within the region of the WLI, at $\Omega \sim 2$ [between Figs. 2(g) and 2(h)]. This mixing was reported by Mace and Hellberg[11] for an $e-e$ plasma, and reverses the previous one. Figure 1 depicts the line where branch mixing takes place. Contrary to the mixing at $v_d > 1$, the mixing at $v_d < 1$ takes place at a wave number far from the most unstable mode (indeed, it involves a stable mode). Therefore, it does not produce any change in the characteristics of the WLI dominant mode, Eq. (9).

Finally, we comment on the $e-e$ acoustic instability.[6] Gary defines it as the two-stream instability (for an $e-e$ plasma) in the domain $v_d \leqslant O(1)$, $\Omega \leqslant O(1)$, and $\Lambda \ll 1$. However, since his analysis is mainly numerical, the boundaries of the instability domain are not defined clearly. The present analysis shows that Gary's instability includes two instability types, the WLI and the WAI, and, in fact, the transition WLI/WAI (at $v_d \sim \Omega$) corresponds to the change of character of the $e-e$ acoustic instability reported by him. Having to deal with two types at a time, Gary uses for $\omega(k)$ hybrid forms of Eqs. (7) and (10), corresponding to the SLI, WLI, and WAI, and computes numerically the maximum

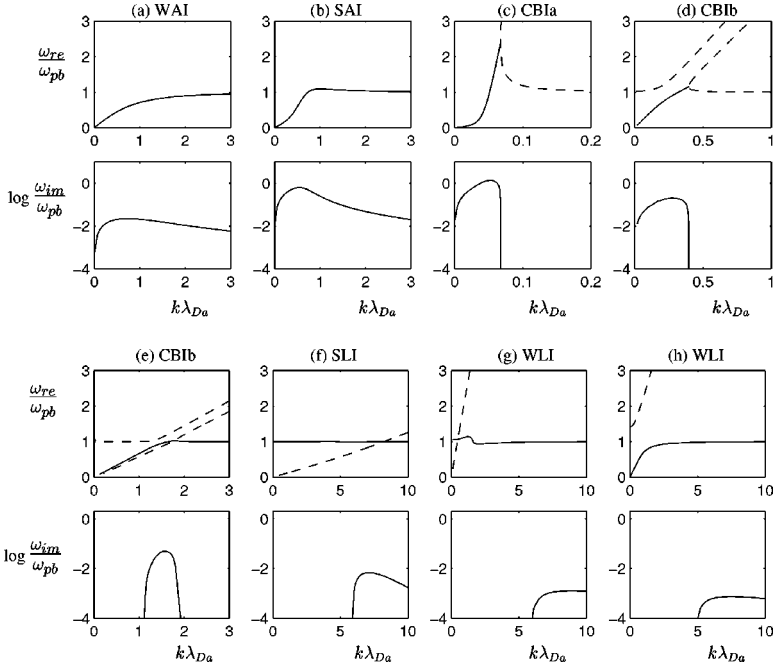

FIG. 2. Solid lines show the evolution of the unstable branch of $\omega(k)$ as the parametric plane (Ω, v_d) is covered clockwise; (a)–(h) correspond to points a–h in Fig. 1. The instability type for each case is given too. Dashed lines correspond to stable branches that interact with the unstable one. Values of (Ω, v_d) are: (a) $(\Omega, v_d) = (0.01, 0.1)$, (b) $(\Omega, v_d) = (0.01, 2)$, (c) $(\Omega, v_d) = (0.1, 20)$, (d) $(\Omega, v_d) = (5, 20)$, (e) $(\Omega, v_d) = (30, 20)$, (f) $(\Omega, v_d) = (30, 5)$, (g) $(\Omega, v_d) = (3, 0.5)$, (h) $(\Omega, v_d) = (1, 0.2)$.

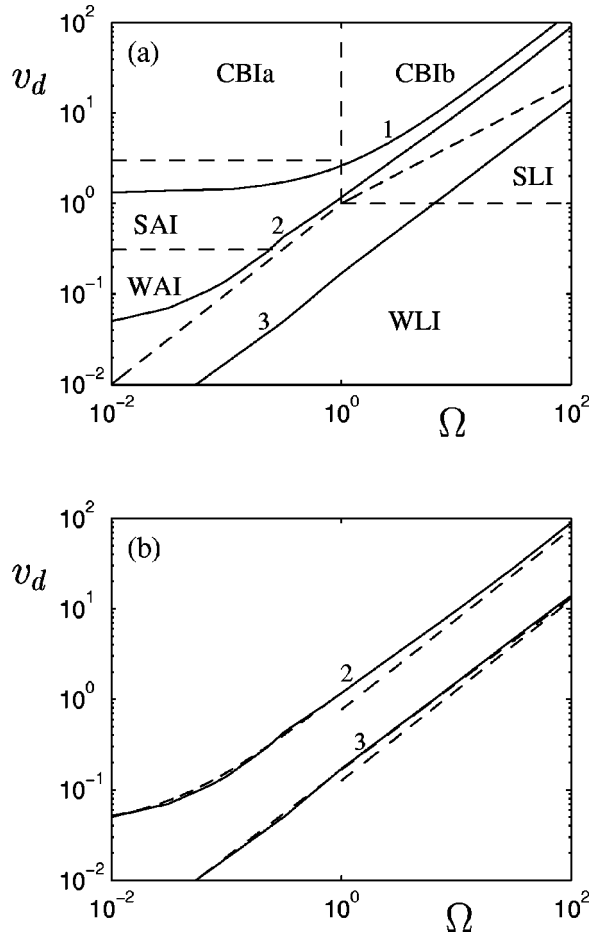

FIG. 3. (a) Instability threshold for $\Lambda^2=1(1)$, $10^{-1}(2)$, and $10^{-3}(3)$; dashed lines reproduce the domains of dominance of Fig. 1. (b) Comparison of the exact threshold with approximate Eqs. (26), (27), and (31).

growth rate. Our analysis gives the distinguished expressions of $\omega(k)$ for the WLI and the WAI and analytical expressions for $\omega_{im}^*(\Omega,v_d)$.

III. THE INSTABILITY THRESHOLD

We have shown that for $\Lambda\to 0$ the threshold velocity for the two-stream velocity is $v_{dt}(\Omega)=0$. For $\Lambda>0$, the last term in Eq. (4) has always a stabilizing effect and, as a consequence, one has $v_{dt}(\Omega,\Lambda)>0$ for $\Lambda>0$.

The threshold function $v_d=v_{dt}(\Omega,\Lambda)$ is the solution of

$$\omega_{im}(k\lambda_{Da},v_d,\Omega,\Lambda)=0,\quad \frac{\partial\omega_{im}}{\partial k}=0, \tag{19}$$

when it corresponds to a mode with $k>0$, and of

$$\omega_{im}=0,\quad k=0, \tag{20}$$

otherwise. Figure 3(a) depicts $v_d=v_{dt}(\Omega,\Lambda)$ for different Λ between 0 and 1, obtained from solving numerically the exact dispersion relation, Eq. (1). The threshold velocity grows with both Λ and Ω. In general, the threshold velocity crosses the regions of the weak acoustic, weak Langmuir, and strong Langmuir instabilities. The domains of the different stability types of the case $\Lambda=0$ remain approximately valid for $\Lambda>0$ above the instability threshold.

For $\Lambda=1$, the threshold function is[1]

$$v_{dt}(\Omega,\Lambda=1)=1.31(1+\Omega),$$

which corresponds to $z_b=-z_a$ and $R_1(z_a)=0$; this result is easily deduced from the symmetry properties of Eq. (1) and $R(z)$. We try next to obtain asymptotic expressions of $v_d=v_{dt}(\Omega,\Lambda)$ for Λ small.

For $\Lambda\ll 1$, we have $|z_b|\gg 1$ and $\gamma(z_b)$, in Eq. (4), can be approximated by Eq. (A3). In addition, the WAI, WLI, and SLI have z_a almost real and $R_2(z_a)\ll k\lambda_{Da}^2+R_1(z_a)$. Making then the appropriate expansions of Eq. (4), the eigenmodes for these three instabilities follow:

$$\omega_{re}\simeq\pm\omega_0[1+O(\Lambda^2)],$$

$$\omega_{im}\simeq-\omega_0\sqrt{\frac{\pi}{8}}\frac{(z_a+v_d)^2}{\Omega^2}f(z_a,v_d,\Omega,\Lambda), \tag{21}$$

with

$$\frac{\omega_0}{\omega_{pb}}=\frac{k\lambda_{Da}}{\sqrt{k^2\lambda_{Da}^2+R_1(z_a)}},$$

$$f(z_a)=z_a\exp\left(-\frac{z_a^2}{2}\right)+\frac{z_a+v_d}{\Lambda^3\Omega}\exp\left(-\frac{(z_a+v_d)^2}{2\Lambda^2\Omega^2}\right). \tag{22}$$

Here z_a, z_b, and $k\lambda_{Da}$ are related through

$$z_b\Lambda\Omega=z_a+v_d\simeq\frac{\Omega}{\sqrt{k^2\lambda_{Da}^2+R_1(z_a)}}. \tag{23}$$

Using Eqs. (21)–(23) and $z_a\neq -v_d$, conditions (19) and (20) are equivalent to

$$f(z_a)=0,\quad \frac{\partial f(z_a)}{\partial z_a}=0,\quad \text{for } k>0, \tag{24}$$

$$f(z_a)=0,\quad k=0, \tag{25}$$

respectively. These equations provide different asymptotic expressions of $v_{dt}(\Omega,\Lambda)$ in the WAI, WLI, and SLI domains. When the threshold velocity lies in SLI domain, the approximate solution of Eq. (24) is $v_d\simeq v_{dt,1}(\Omega,\Lambda)$ with $v_{dt,1}$ given parametrically by

$$v_{dt,1}(\Lambda,z_b^*)=z_b^*\Lambda\Omega(\Lambda,z_b^*),$$

$$\Omega(\Lambda,z_b^*)=\Lambda^{-1}(z_b^*-\sqrt{1+2\ln(z_b^*/\Lambda^2)})^{-1}, \tag{26}$$

with z_b^* a convenient parameter. When the threshold velocity lies in the WLI domain, the approximate solution of Eq. (24) is $v_d\simeq v_{dt,2}(\Omega,\Lambda)$ with $v_{dt,2}$ given parametrically by

$$v_{dt,2}(\Lambda,z_b^*)=\Lambda^{-2}z_b^{*3}\exp(-z_b^{*2}/2),$$

$$\Omega(\Lambda,z_b^*)=\Lambda^{-3}(z_b^{*2}-1)\exp(-z_b^{*2}/2). \tag{27}$$

Simpler, explicit expressions of the above two threshold functions are

$$\frac{v_{dt,1}}{\Omega}\simeq\Lambda\sqrt{-4\ln\Lambda}+O(\ln\Lambda), \tag{28}$$

$$\frac{v_{dt,2}}{\Omega}\simeq\Lambda\sqrt{-2\ln\Lambda^3\Omega}+O(\ln\Lambda). \tag{29}$$

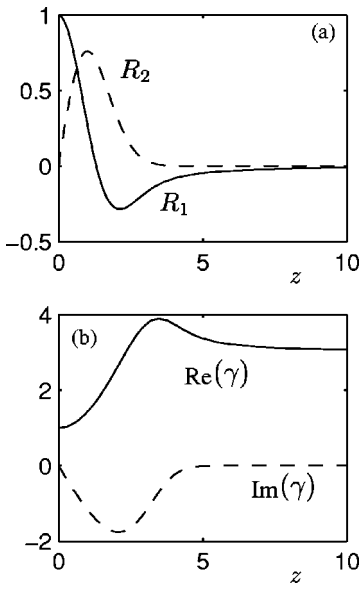

FIG. 4. (a) Real (solid line) and imaginary part (dashed line) of the dispersion function $R(z)$ for z real. (b) Real (solid line) and imaginary part (dashed line) of $\gamma(z)$ for z real.

Equation (27) is valid while $\omega_{im}^{*}=0$ occurs for $k^{*}>0$, which means

$$z_b^{*}=\frac{1}{\Lambda\sqrt{1+k^{*2}\lambda_{Da}^2}}<\frac{1}{\Lambda},$$

or, using Eq. (27),

$$\Omega>\Omega_0(\Lambda)\equiv\frac{1-\Lambda^2}{\Lambda^5}\exp\left(-\frac{1}{2\Lambda^2}\right). \tag{30}$$

For $\Omega<\Omega_0$, the threshold velocity comes from solving Eq. (25). Since $v_{dt,2}(\Omega_0)\simeq\Omega_0$, the transition from conditions (24) to (25), corresponds to the WLI/WAI transition. The solution of Eq. (25) within the WAI domain is

$$v_d=v_{dt,3}(\Omega,\Lambda)$$
$$=(3\Lambda^2+1)^{1/2}\left[\Omega+\frac{1}{\Lambda^3}\exp\left(-\frac{1}{2\Lambda^2}-\frac{3}{2}-3\Lambda^2\right)\right]. \tag{31}$$

Figure 3(b) compares the exact threshold velocity with analytical expressions (26), (27), and (31), showing that the agreement is very good. As far as we have checked, Eqs. (26) and (27) are original; Papadopoulos[5] and Kindel and Kennel[14] proposed the simplified expression of $v_{dt,2}$ in Eq. (29), but Papadopoulos omitted the first factor Λ in the right-hand side, and Kindel and Kennel the cubic exponent of Λ within the square root. Jackson[1] found a simplified expression of $v_{dt,3}(\Omega,\Lambda)$ for $\Lambda\ll 1$; and Papadopoulos[5] proposed Eq. (31) without the two terms with $3\Lambda^2$. These terms, which have a non-negligible effect, come from a corrected expression of the Landau damping by McKinstrie *et al.*[16]

IV. CONCLUSIONS

We have shown that a complete description of the different types of the two-stream instability in the (v_d,Ω) plane, for oscillations involving two plasma species only, is obtained from a systematic asymptotic analysis of the dispersion relation for the zero-Debye-length-ratio limit. The study is applicable, at least, to ion–electron plasmas and electron–electron plasmas (with a frozen ion population providing quasineutrality), and provides equivalences between instabilities in both plasmas.

In contrast to numerical analyses, our asymptotic study has allowed us (i) to determine clearly the region of dominance of the different instability types, (ii) to explain their dominant character (Langmuir, acoustic, or reactive) and the transitions between two neighboring types, and (iii) to derive simple expressions for the maximum growth rate. The contributions on the weak Langmuir instability and its transition to the weak acoustic and strong Langmuir instabilities, are specially relevant since they were more poorly known. Also, the relation between the branch mixing at the CBI/SLI transition and within the WLI have been discussed.

For the case of a small Debye length ratio, new analytical expressions of the threshold function have been obtained for the cases of the weak and strong Langmuir instabilities, and an improved expression has been proposed for the threshold of the weak acoustic instability.

The analysis presented here is valid when the current-driven instability is governed by the interaction of two-species only. Current-driven instabilities in multiple-species plasmas, like those formed around strong double layers, will be presented in another paper.

ACKNOWLEDGMENTS

We thank Professor M. Martínez-Sánchez for his valuable remarks on the manuscript.

This research was supported by Ministerio de Educación y Cultura of Spain under Project No. PB97-0574-C04-02.

APPENDIX: PLASMA PERTURBATION RESPONSE

In a collisionless, homogeneous, Maxwellian plasma, the response in density n and pressure p of a certain species α to small planar perturbations on the electrostatic potential ϕ can be written as[10]

$$\frac{n_{\alpha 1}}{n_\alpha}=-\frac{q_\alpha\phi_1}{T_\alpha}R(z_\alpha),\quad \frac{p_{\alpha 1}}{p_\alpha}=\gamma(z_\alpha)\frac{n_{\alpha 1}}{n_\alpha}, \tag{A1}$$

where $T_\alpha=p_\alpha/n_\alpha$,

$$z_\alpha=\frac{\omega-\mathbf{k}\cdot\mathbf{V}_\alpha}{kc_\alpha}$$

is the relative phase velocity of the perturbation with respect to species α (with $\mathbf{V}_\alpha$ the species drift velocity and $c_\alpha=\sqrt{T_\alpha/m_\alpha}$),

$$\gamma(z)=z^2+R^{-1}(z) \tag{A2}$$

measures the species thermodynamic response to that perturbation, and $R(z)$ is the plasma dispersion function.[17] For a Maxwellian distribution function, one has $R(z)=R_1(z)+iR_2(z)$ with

$$R_1(z)=1-z\exp(-z^2/2)\int_0^z \exp(y^2/2)dy,$$

$$R_2(z)=\sqrt{\pi/2}\; z\exp(-z^2/2).$$

Figure 4 shows $R(z)$ and $\gamma(z)$ for z real, when $R_1(z)$ and $R_2(z)$ are real, and contributions to R_2 and the imaginary part of $\gamma(z)$ come entirely from Landau resonance. Some useful results are $R_1(-z)=R_1(z)$ and $R_2(z)=-R_2(z)$; $R_1(z)$ crosses 0 at $z\simeq 1.31$; $R_1=1-z^2+O(z^4)$ for $|z|\ll 1$; $R_1=-z^{-2}-3z^{-4}+O(z^{-6})$ for $|z|\gg 1$; and

$$\gamma(z)\simeq[3+O(z^{-2})]-\mathrm{i}\left[\sqrt{\frac{\pi}{2}}[z^5+O(z^3)]\exp\left(-\frac{z^2}{2}\right)\right], \tag{A3}$$

for $|z|\gg 1$.

[1] E. A. Jackson, Phys. Fluids **3**, 786 (1960).
[2] A. Krall and A. Trivelpiece, *Principles of Plasma Physics* (San Francisco Press, San Francisco, 1986).
[3] O. Buneman, Phys. Rev. **115**, 503 (1959).
[4] D. B. Melrose, *Instabilities in Space and Laboratory Plasmas* (Cambridge University Press, Cambridge, 1986).
[5] K. Papadopoulos, Rev. Geophys. Space Phys. **15**, 113 (1977).
[6] S. P. Gary, Phys. Fluids **30**, 2745 (1987).
[7] T. M. O'Neil and J. H. Malmberg, Phys. Fluids **11**, 1754 (1968).
[8] I. H. Cairns, Phys. Fluids B **1**, 204 (1989).
[9] T. E. Stringer, J. Nucl. Energy, Part C **6**, 267 (1964).
[10] E. Ahedo and V. Lapuerta, Phys. Plasmas **8**, 3873 (2001).
[11] R. L. Mace and M. A. Hellberg, J. Plasma Phys. **43**, 239 (1990).
[12] R. Penrose, Phys. Fluids **3**, 258 (1960).
[13] B. D. Fried and R. W. Gould, Phys. Fluids **4**, 139 (1961).
[14] J. M. Kindel and C. F. Kennel, J. Geophys. Res. **76**, 3055 (1971).
[15] S. P. Gary, *Theory of Space Plasma Microinstabilities* (Cambridge University Press, New York, 1993).
[16] C. J. McKinstrie, R. E. Giacone, and E. A. Startsev, Phys. Plasmas **6**, 463 (1999).
[17] S. Ichimaru, *Statistical Plasma Physics* (Addison–Wesley, Redwood City, 1992).